

DisFaceRep: Representation Disentanglement for Co-occurring Facial Components in Weakly Supervised Face Parsing

Xiaoqin Wang

School of Computer Science and
Software Engineering, Shenzhen
University
Shenzhen, China
wangxiaoqin2022@email.szu.edu.cn

Xianxu Hou*

School of AI and Advanced
Computing, Xi'an Jiaotong-Liverpool
University
Suzhou, China
hxianxu@gmail.com

Meidan Ding

School of Computer Science and
Software Engineering, Shenzhen
University
Shenzhen, China
dingmeidan2023@email.szu.edu.cn

Junliang Chen

Department of Electrical and
Electronic Engineering, The Hong
Kong Polytechnic University
Hong Kong, China
jun-liang.chen@connect.polyu.hk

Kaijun Deng

School of Computer Science and
Software Engineering, Shenzhen
University
Shenzhen, China
dengkaijun2023@email.szu.edu.cn

Jinheng Xie

Department of Electrical and
Computer Engineering, National
University of Singapore
Singapore, Singapore
sierkinhane@gmail.com

Linlin Shen*

Computer Vision Institute, School of
Artificial Intelligence, Shenzhen
University
Guangdong Provincial Key
Laboratory of Intelligent Information
Processing, Shenzhen University
Shenzhen, China
llshen@szu.edu.cn

Abstract

Face parsing aims to segment facial images into key components such as eyes, lips, and eyebrows. While existing methods rely on dense pixel-level annotations, such annotations are expensive and labor-intensive to obtain. To reduce annotation cost, we introduce Weakly Supervised Face Parsing (WSFP), a new task setting that performs dense facial component segmentation using only weak supervision, such as image-level labels and natural language descriptions. WSFP introduces unique challenges due to the high co-occurrence and visual similarity of facial components, which lead to ambiguous activations and degraded parsing performance. To address this, we propose DisFaceRep, a representation disentanglement framework designed to separate co-occurring facial components through both explicit and implicit mechanisms. Specifically, we introduce a co-occurring component disentanglement strategy to explicitly reduce dataset-level bias, and a text-guided component disentanglement

loss to guide component separation using language supervision implicitly. Extensive experiments on CelebAMask-HQ, LaPa, and Helen demonstrate the difficulty of WSFP and the effectiveness of DisFaceRep, which significantly outperforms existing weakly supervised semantic segmentation methods. The code will be released at <https://github.com/CVI-SZU/DisFaceRep>.

CCS Concepts

• Computing methodologies → Image representations.

Keywords

Face Parsing, Weakly Supervised Learning, Visual Language Models

ACM Reference Format:

Xiaoqin Wang, Xianxu Hou, Meidan Ding, Junliang Chen, Kaijun Deng, Jinheng Xie, and Linlin Shen. 2025. DisFaceRep: Representation Disentanglement for Co-occurring Facial Components in Weakly Supervised Face Parsing. In *Proceedings of the 33rd ACM International Conference on Multimedia (MM '25)*, October 27–31, 2025, Dublin, Ireland. ACM, New York, NY, USA, 10 pages. <https://doi.org/10.1145/3746027.3755285>

1 Introduction

Face parsing, a fine-grained semantic segmentation task, aims to assign pixel-level labels to facial images by distinguishing key components such as the eyes, nose, lips, hair, and ears. Accurate facial component segmentation is critical for a wide range of downstream applications, including face swapping [38], face editing [20], face completion [23], and virtual makeup synthesis [39]. Thanks to the

*Corresponding authors

Permission to make digital or hard copies of all or part of this work for personal or classroom use is granted without fee provided that copies are not made or distributed for profit or commercial advantage and that copies bear this notice and the full citation on the first page. Copyrights for components of this work owned by others than the author(s) must be honored. Abstracting with credit is permitted. To copy otherwise, or republish, to post on servers or to redistribute to lists, requires prior specific permission and/or a fee. Request permissions from permissions@acm.org.
MM '25, Dublin, Ireland.

© 2025 Copyright held by the owner/author(s). Publication rights licensed to ACM.
ACM ISBN 979-8-4007-2035-2/2025/10
<https://doi.org/10.1145/3746027.3755285>

availability of densely annotated datasets, existing methods based on Convolutional Neural Networks (CNNs) [11, 28, 30, 35, 51, 72, 73] and, more recently, Transformers [37], have achieved impressive performance. However, creating pixel-level annotations, especially for small and intricate facial features, is time-consuming and not scalable to large datasets or diverse domains.

To alleviate the cost of dense annotations, weakly supervised learning has emerged as a compelling alternative in the semantic segmentation community, formalized as Weakly Supervised Semantic Segmentation (WSSS). It aims to predict pixel-level segmentation masks using only weak supervision signals, including image-level labels [2, 41, 42], bounding boxes [6, 40], point annotations [3], scribbles [25, 53], or natural language descriptions [59]. Despite relying on coarse supervision, recent approaches [14, 15, 57] have achieved performance competitive with, and in some cases exceeding, that of fully supervised methods—highlighting the remarkable potential of weak supervision for dense prediction tasks.

While weakly supervised learning has achieved notable success in general semantic segmentation, it remains largely underexplored in the context of face parsing. To bridge this gap, we propose Weakly Supervised Face Parsing (WSFP), a new task that extends the WSSS paradigm to the facial domain by enabling dense component segmentation under weak annotations. A natural baseline for WSFP is to directly apply existing WSSS methods; however, this proves suboptimal due to challenges unique to WSFP, particularly the difficulty in generating accurate Facial Component Activation Maps (FCAMs). Unlike general semantic segmentation, WSFP suffers from significant activation overlap due to the frequent co-occurrence and high visual similarity of facial components, which degrades the quality of pseudo labels. This issue manifests in two forms: (1) intra-dataset co-occurrence: datasets like CelebAMask-HQ exhibit high co-occurrence of facial categories (e.g., skin and nose appear in nearly every facial image), reducing the discriminative capacity of classification models, as shown in Fig. 1(c); and (2) intra-image co-occurrence: facial components often share similar visual features (e.g., texture and shape) but differ in spatial location (e.g., left vs. right eyes), causing over-activation of visually similar but semantically unrelated regions, as shown in Fig. 1(d). These two forms of co-occurrence present core challenges in WSFP and significantly limit the effectiveness of applying WSSS methods to facial data.

To address these challenges, we propose DisFaceRep (Fig. 2), a novel representation disentanglement framework tailored to the WSFP task. DisFaceRep is built upon two complementary modules: Co-occurring Component Disentanglement (CCD) and Text-guided Component Disentanglement (TCD). CCD explicitly mitigates dataset-level bias by randomly masking dominant facial regions that frequently co-occur using Grounding DINO [32]. This prevents the model from over-relying on high-frequency components during learning. On the other hand, TCD implicitly enhances component separation by aligning visual and textual representations through the facial language pretraining model FLIP [22]. It leverages both positive and negative text-component associations to guide fine-grained activation and suppress semantically unrelated regions. By combining these two strategies, DisFaceRep generates high-quality Facial Component Activation Maps (FCAMs), significantly improving parsing performance under weak supervision. The main contributions of this work are as follows:

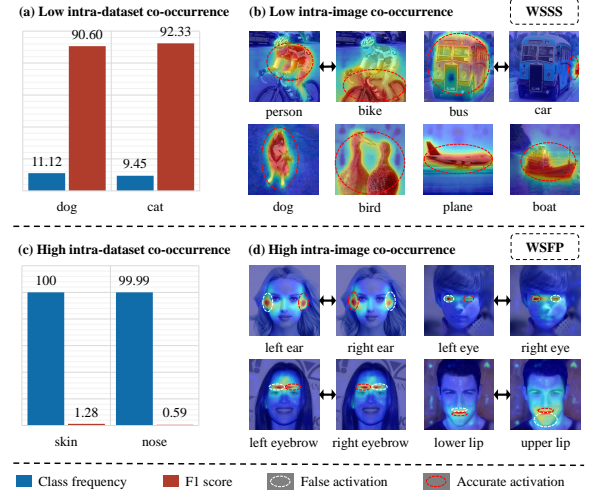


Figure 1: Comparison of co-occurrence challenges in WSSS and WSFP. (a-b) PASCAL VOC [9] shows low intra-dataset and intra-image co-occurrence, along with high inter-class dissimilarity, resulting in high F1 scores. In contrast, (c-d) CelebAMask-HQ [20] exhibits high intra-dataset and intra-image co-occurrence of visually similar facial components, such as skin, nose, ears, eyes, eyebrows, and lips. This frequent co-occurrence and visual similarity of components lead to false activations and low F1 scores when WSSS methods [62] are directly applied.

- We introduce WSFP, a new task that extends WSSS to facial component parsing. We identify and analyze the core challenges of frequent co-occurrence and visual similarity, which limit the effectiveness of directly applying existing WSSS’s methods to WSFP.
- We propose DisFaceRep, a representation disentanglement framework that addresses these challenges through two complementary modules: Co-occurring Component Disentanglement, which explicitly reduces dataset-level bias, and Text-guided Component Disentanglement, which implicitly guides component separation via vision-language alignment.
- We conduct extensive experiments on CelebAMask-HQ, LaPa, and Helen, demonstrating that DisFaceRep significantly outperforms state-of-the-art WSSS methods in both segmentation accuracy and component-level precision.

2 Related Works

2.1 Fully Supervised Face Parsing

With the advancement of deep learning, numerous fully supervised methods have been developed for face parsing, which can be broadly categorized into global-based and local-based approaches.

Global-based methods aim to predict pixel-wise labels for the entire face image using features extracted from convolutional or graph-based networks. Early CNN-based models [12, 26, 30, 55, 72] directly learn from RGB inputs to capture spatial relationships among facial regions. More recent efforts incorporate structural priors: AGRNet [50] and EAGRNet [51] utilize graph representations and edge information to enhance spatial consistency, while

DML-CSR [69] combines dual graph convolutional networks with cyclic self-regulation to handle noisy labels. FP-LIIF [46] proposes a local implicit function to exploit facial symmetry and continuity. In addition, FaRL [70] explores large-scale vision-language pretraining on facial data to boost downstream tasks such as face parsing.

Local-based methods, by contrast, decompose the parsing task into separate sub-networks, each dedicated to a specific facial region. Luo et al. [36] adopt a hierarchical network that segments each facial part individually. Zhou et al. [73] propose an interlinked CNN model that performs post-detection pixel classification, albeit with high memory and computation cost. Liu et al. [29] introduce a two-stage method combining a shallow CNN and spatial RNN to balance accuracy and inference speed. Despite the remarkable progress of both paradigms, they all rely heavily on dense pixel-level labels, which are expensive and time-consuming to obtain.

2.2 Weakly Supervised Semantic Segmentation

Weakly supervised semantic segmentation aims to reduce annotation costs by training models with weak supervision, such as image-level labels. The standard WSSS pipeline typically follows a three-stage process: (1) a classification network is trained using weak labels to generate Class Activation Maps (CAMs) [71]; (2) these initial CAMs are refined into pseudo masks using post-processing methods such as dense CRF [17], pixel affinity propagation [1, 2], or saliency-based techniques [13, 34]; and (3) the refined pseudo masks are used to supervise a segmentation network.

Due to the discriminative nature of classification models, CAMs typically highlight only the most salient object regions. To address this limitation, various methods have been proposed to enhance CAM completeness. These include cross-image attention [21, 49], adversarial erasing [18, 19, 64, 68], consistency regularization through data augmentation [54, 67], boundary-aware refinement [10, 16, 44], loss function modification [5, 56], and Transformer-based approaches [45, 60, 61]. Recently, vision-language pretraining, particularly CLIP, has gained traction in WSSS. CLIMS [59] first introduced CLIP to improve object region activation. CLIP-ES [27] enhances CAM quality using text prompts and GradCAM [47], while WeakCLIP [74] proposes a fine-grained text-to-pixel alignment paradigm. WeCLIP [65] further explores a single-stage approach leveraging a frozen CLIP backbone for CAM refinement.

These methods demonstrate the effectiveness of weak supervision for semantic segmentation in general domains, particularly by improving CAM quality. However, face parsing under weak supervision remains largely underexplored. In this work, we analyze the unique challenges of weakly supervised learning in the face parsing setting and introduce a novel task and framework tailored for low-cost, fine-grained facial segmentation.

3 Methodology

3.1 Problem Definition and Key Challenges

In this section, we formally define the Weakly Supervised Face Parsing (WSFP) setting. Given a training set $\mathcal{D} = \{x_i, y_i\}_{i=1}^n$, where $x_i \in \mathcal{X}$ represents the i -th face image and $y_i \in \mathcal{Y}$ denotes its corresponding image-level label, the objective of WSFP is to segment a face image x into K facial components using only the weak supervisory signal y . In contrast to the WSSS paradigm, the WSFP pipeline

consists of two stages: first, a face component classification model is trained to generate Facial Component Activation Maps (FCAMs) under weak supervision, and then pseudo masks are generated by setting a threshold θ on FCAMs; second, these pseudo masks are used as dense supervision to train a face parsing model.

Among the two stages in the WSFP pipeline, generating accurate and complete FCAMs is the most critical and challenging step. A key obstacle is the strong co-occurrence among facial components, which hinders the model's ability to distinguish and localize them accurately. This challenge arises in two main forms. First, there is intra-dataset co-occurrence, where certain facial components co-occur in a large majority of training images. As shown in Fig.1(c), components such as skin and nose appear in over 99% of images in the dataset, leading to high class frequency and poor discriminability across components. Second, the human face exhibits strong intra-image co-occurrence, with components that have similar appearance but distinct spatial positions (e.g., left/right eyes and eyebrows). As illustrated in Fig.1(d), traditional classification networks tend to over-activate such components, resulting in ambiguous localization. These two forms of co-occurrence and visual similarity significantly degrade the quality of FCAMs, thereby limiting the performance of face parsing. To address this, we propose DisFaceRep, a representation disentanglement framework designed to resolve component entanglement under weak supervision.

3.2 Overview of DisFaceRep

The overall framework of DisFaceRep is depicted in Fig. 2. Given a training set $\mathcal{D} = \{x_i, y_i\}_{i=1}^n$, our method first applies Co-occurring Component Disentanglement (CCD) to suppress high-frequency facial components explicitly. This is achieved by randomly masking regions associated with frequently co-occurring attributes, resulting in a new training set $\hat{\mathcal{D}} = \{\hat{x}_i, \hat{y}_i\}_{i=1}^n$, where \hat{x}_i and \hat{y}_i denote the images and labels with reduced co-occurrence bias. Following [60], we adopt a multi-class token ViT [8] as the backbone, and feed \hat{x} into it to extract class tokens $F_{cls} \in \mathbb{R}^{K \times d}$ and patch tokens $F_{pat} \in \mathbb{R}^{N \times d}$, where K and N represent the number of categories and image patches, and d is the embedding dimension. An MLP-based projector transforms the class tokens into a vision-language space, while patch tokens are reshaped and passed through a convolutional layer and a sigmoid function. The resulting feature map P_k is element-wise multiplied with \hat{x} to extract foreground facial component feature v_{ffc}^k , while background component feature v_{bfc}^k is computed by multiplying $(1 - P_k)$ with \hat{x} . To further enhance component separation, we introduce Text-guided Component Disentanglement (TCD), which leverages FLIP [22]—a face-specific vision-language model built upon CLIP [43]—for implicitly aligning visual features with semantic concepts. Finally, we extract accurate and complete FCAMs from the trained classification network following the procedure in [60].

3.3 Co-occurring Component Disentanglement

Formally, CCD leverages the Grounding DINO [31], which is an open-set object detection method, to randomly mask some facial components based on predicted bounding boxes. Due to the presence of multiple similar facial components, relying solely on the highest-confidence bounding box for coordinate prediction

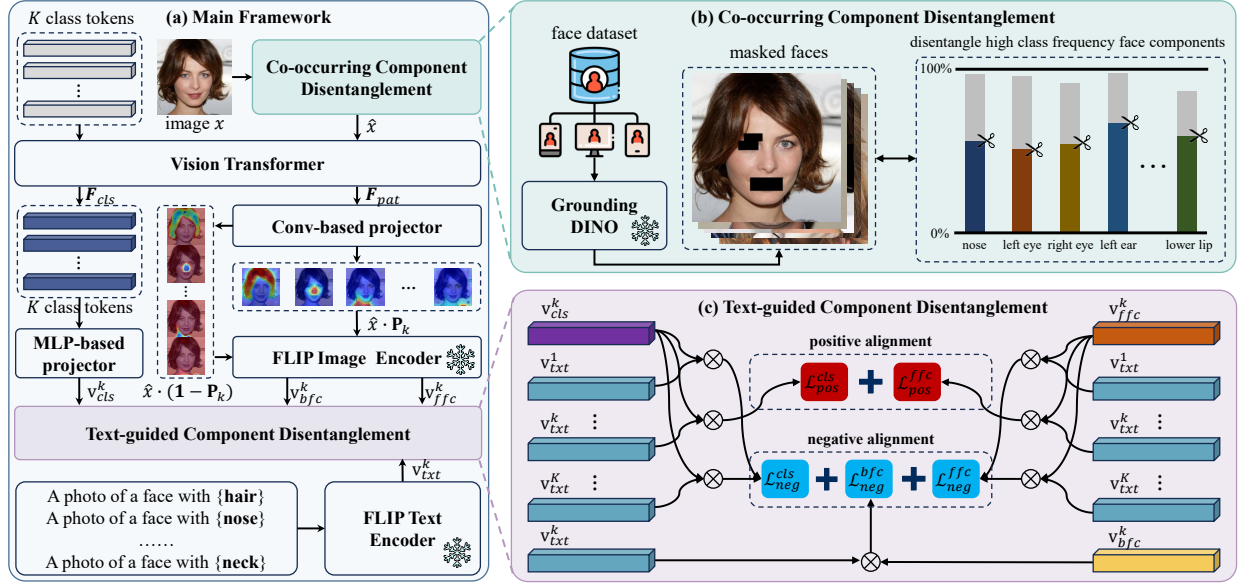


Figure 2: An overview of our proposed DisFaceRep for WSFP. (a) The main framework for predicting initial FCAMs. v_{cls}^k , v_{ffc}^k , v_{bfc}^k , and v_{txt}^k are the k -th representations corresponding to the class token, foreground facial component, background facial component, and text description, respectively. $\hat{x} \cdot P_k$ and $\hat{x} \cdot (1 - P_k)$ are FCAMs for the foreground and background, respectively. (b) Co-occurring component disentanglement explicitly suppresses dominant facial components via the frozen Grounding DINO [31] model. (c) Text-guided component disentanglement implicitly separates component representations via positive alignment (\mathcal{L}_{pos}^{cls} and \mathcal{L}_{pos}^{ffc}) and negative alignment (\mathcal{L}_{neg}^{cls} , \mathcal{L}_{neg}^{ffc} , and \mathcal{L}_{neg}^{bfc}). \otimes denotes cosine similarity.

may yield inaccurate results. To solve this problem, we design a multi-threshold filtering strategy to obtain a set of accurate prediction boxes. Specifically, there is a set of candidate coordinates $B^i = [h_1^i, w_1^i, h_2^i, w_2^i]$, $i \in \{1, 2, \dots, m\}$ with the highest confidence for a set of facial components that are masked out. The condition for the accurate prediction box of the i -th masked component is:

$$C^i = \begin{cases} \text{True} \cap \left(\frac{w_1^i + w_2^i}{2} < \frac{W}{2} \right), & \text{if right components} \\ \text{True} \cap \left(\frac{w_1^i + w_2^i}{2} > \frac{W}{2} \right), & \text{if left components} \\ \text{True}, & \text{otherwise} \end{cases} \quad (1)$$

where W is the width of the image. The pixel coordinate position set of the face components with high category frequency is $M = \bigcup_{i=1}^m \{B_i | C_i\}$. Finally, we can accurately mask out some components with high class frequency as follows:

$$\hat{x}(i, j) = \begin{cases} 0, & \text{if } (i, j) \in M \\ x(i, j), & \text{otherwise} \end{cases} \quad (2)$$

where $x(i, j)$ is the pixel value of the face image x . The \hat{y} corresponds to the image label of \hat{x} . In this work, the candidate set of facial components that may be masked out in the image is “nose, left/right eye, left/right eyebrow, left/right ear, and mouth”. These components are high-frequency, cover common face parsing datasets, and have no overlap between boxes of different components. Therefore, masking out in the facial images can mitigate dataset-level bias.

3.4 Text-guided Component Disentanglement

After applying CCD, we obtain a new training set $\hat{\mathcal{D}} = \{\hat{x}_i, \hat{y}_i\}_{i=1}^n$ with reduced high class frequency and lower co-occurrence bias. As shown in Fig. 2, the k -th class token and \hat{x} are input to the ViT backbone, and then obtain the class embedding F_{cls}^k and patch embedding F_{pat}^k . Then, F_{cls}^k is projected into the class representation v_{cls}^k via an MLP-based projector:

$$v_{cls}^k = W^T F_{cls}^k \quad (3)$$

where W is projection matrix. Thus, each class representation vector corresponds to distinct facial semantic information.

In addition, a convolutional layer and a sigmoid function $\sigma(\cdot)$ are directly applied to the patch token F_{pat}^k and generate the patch attention map P_k :

$$P_k = \sigma \left(\text{conv} \left(F_{pat}^k \right) \right) \quad (4)$$

To enable text-guided facial component disentanglement, we use the image encoder $\varepsilon_v(\cdot)$ from the facial domain CLIP, i.e., FLIP [22] to generate both the foreground and background facial component representation vectors:

$$v_{ffc}^k = \varepsilon_v(\hat{x} \cdot P_k) \quad (5)$$

$$v_{bfc}^k = \varepsilon_v(\hat{x} \cdot (1 - P_k)) \quad (6)$$

where v_{ffc}^k is the k -th foreground facial component representation vector, and v_{bfc}^k is the k -th background facial component representation vector.

To disentangle entangled facial components using text supervision, we construct a text prompt T_k , i.e., ‘a photo of a face with {component}’, e.g., ‘a photo of a face with nose’, following FLIP [22]. Then, the text encoder $\varepsilon_t(\cdot)$ from FLIP is utilized to obtain the text representation vector \mathbf{v}_{txt}^k of the k -th text prompt:

$$\mathbf{v}_{txt}^k = \varepsilon_t(T_k) \quad (7)$$

Finally, based on the \mathbf{v}_{cls}^k , \mathbf{v}_{ffc}^k , \mathbf{v}_{bfc}^k , and \mathbf{v}_{txt}^k , the proposed TCD implicitly disentangles different facial components through the following positive and negative alignment losses.

3.4.1 Positive Alignment. It aims to pull facial component features close to the corresponding text representations. Specifically, given the k -th class representation \mathbf{v}_{cls}^k and its corresponding text representation \mathbf{v}_{txt}^k , we begin by calculating the cosine similarity between \mathbf{v}_{cls}^k and \mathbf{v}_{txt}^k , and then the positive loss in terms of class representation \mathcal{L}_{pos}^{cls} is:

$$\mathcal{L}_{pos}^{cls} = - \sum_{k=1}^K \hat{y}_k \cdot \log \left(\text{sim} \left(\mathbf{v}_{cls}^k, \mathbf{v}_{txt}^k \right) \right) \quad (8)$$

where $\text{sim}(\cdot)$ indicates the cosine similarity.

To improve the completeness of activated component regions, we also encourage the model to maintain the feature consistency of \mathbf{v}_{ffc}^k and \mathbf{v}_{txt}^k . Thus, we design the foreground component and the text prompt matching loss \mathcal{L}_{pos}^{ffc} as:

$$\mathcal{L}_{pos}^{ffc} = - \sum_{k=1}^K \hat{y}_k \cdot \log \left(\text{sim} \left(\mathbf{v}_{ffc}^k, \mathbf{v}_{txt}^k \right) \right) \quad (9)$$

Thus, the positive alignment consists of \mathcal{L}_{pos}^{cls} and \mathcal{L}_{pos}^{ffc} as:

$$\mathcal{L}_{pos} = \alpha_0 \mathcal{L}_{pos}^{cls} + \alpha_1 \mathcal{L}_{pos}^{ffc} \quad (10)$$

where α_0 and α_1 are weighting coefficients. By maximizing \mathcal{L}_{pos} , the model is encouraged to focus on discriminative regions associated with each facial component.

3.4.2 Negative Alignment. Due to frequently co-occurring and visually similar components, the classification model trained only with \mathcal{L}_{pos} often over-activates non-target regions. To mitigate this, we introduce three negative losses that explicitly suppress spurious activations and promote better component separation.

Specifically, given the class representation \mathbf{v}_{cls}^k and the l -th non-corresponding text representation $\mathbf{v}_{txt}^{k,l}$, the \mathcal{L}_{neg}^{cls} is used to suppress the co-occurring components in the class representation space as:

$$\mathcal{L}_{neg}^{cls} = - \sum_{k=1}^K \sum_{l=1}^L \hat{y}_k \cdot \log \left(1 - \text{sim} \left(\mathbf{v}_{cls}^k, \mathbf{v}_{txt}^{k,l} \right) \right) \quad (11)$$

To further suppress co-occurring facial components, we design the \mathcal{L}_{neg}^{ffc} loss for disentangling the \mathbf{v}_{ffc}^k from the l -th non-corresponding text representation $\mathbf{v}_{txt}^{k,l}$:

$$\mathcal{L}_{neg}^{ffc} = - \sum_{k=1}^K \sum_{l=1}^L \hat{y}_k \cdot \log \left(1 - \text{sim} \left(\mathbf{v}_{ffc}^k, \mathbf{v}_{txt}^{k,l} \right) \right) \quad (12)$$

We also introduce the background region and text representation matching loss \mathcal{L}_{neg}^{bfc} to account for broader contextual information and reduce false activations:

$$\mathcal{L}_{neg}^{bfc} = - \sum_{k=1}^K \hat{y}_k \cdot \log \left(1 - \text{sim} \left(\mathbf{v}_{bfc}^k, \mathbf{v}_{txt}^k \right) \right) \quad (13)$$

Finally, we combine the above negative losses as follows:

$$\mathcal{L}_{neg} = \beta_0 \mathcal{L}_{neg}^{cls} + \beta_1 \mathcal{L}_{neg}^{ffc} + \beta_2 \mathcal{L}_{neg}^{bfc} \quad (14)$$

where β_0 , β_1 , and β_2 are weighting coefficients. Minimizing \mathcal{L}_{neg} encourages the model to suppress irrelevant activations and better disentangle complete and distinct facial components.

3.4.3 Activation Regularization. Following [59], DisFaceRep incorporates the activation regularization loss for ensuring that the irrelevant backgrounds are excluded in the activation map \mathbf{P}_k :

$$\mathcal{L}_{reg} = \frac{1}{K} \sum_{k=1}^K S_k, \quad S_k = \frac{1}{HW} \sum_{h=1}^H \sum_{w=1}^W \mathbf{P}_k(h, w) \quad (15)$$

where S_k is the activation area of the k -th facial component, and H is the height of the image.

3.4.4 Overall Objective. The overall training objective of the proposed DisFaceRep framework integrates both alignment and regularization losses and is defined as:

$$\mathcal{L} = \mathcal{L}_{pos} + \mathcal{L}_{neg} + \lambda \mathcal{L}_{reg} \quad (16)$$

where λ is the hyper-parameter weighting the three loss terms.

4 Experiments

4.1 Experimental Settings

4.1.1 Datasets and Evaluation Metrics. We conduct experiments on three standard face parsing datasets: CelebAMask-HQ [20], LaPa [33], and Helen [48]. CelebAMask-HQ contains 30,000 images, split into 24,183 for training, 2,993 for validation, and 2,824 for testing, with annotations for 19 classes, including background, skin, eyes, eyebrows, nose, mouth, lips, hair, ears, accessories, and clothing. To evaluate the performance of pseudo masks, we uniformly sampled 3,820 samples from the training set, forming a representative training subset. LaPa consists of 18,176 training images, 2,000 validation images, and 2,000 testing images, and is annotated for 11 classes, including background, skin, hair, nose, mouth, eyes, eyebrows, and lips. Helen contains 2,330 images with the same 11 labels as LaPa. It is split into 2,000, 230, and 100 images for training, validation, and testing. For evaluation, we report the mean F1 score across all facial categories, excluding the background.

4.1.2 Implementation Details. Our proposed DisFaceRep adopts the Vision Transformer DeiT-S [52] with multi-class tokens as the backbone and initializes the model with ImageNet-pretrained weights [7]. Following the training setup in [60], we use the AdamW optimizer with an initial learning rate of 5×10^{-6} and a batch size of 36. Input images are resized to 448×448 . The loss weighting coefficients $[\alpha_0, \alpha_1, \beta_0, \beta_1, \beta_2, \lambda]$ are set to $[1.2, 0.2, 2.1, 0.1, 0.017, 0.05]$. During the pseudo-label generation phase, we remove Grounding DINO [32] and FLIP [22], and follow the [60] method to obtain



Figure 3: Qualitative comparison of FCAMs for frequently co-occurring and visually similar facial components (left/right (l-/r-)eye/brow/ear, upper/lower (u-/l-)lip, skin, nose, mouth, hair, and neck) in the CelebAMask-HQ dataset.

FCAMs. Then, we set the threshold θ to 0.5 to generate pseudo-labels. For the face parsing model, we adopt DeepLab-V1 [24] with ResNet38 [58] as the backbone. Notably, we omit CRF post-processing [4] during inference. Additionally, CLIP [43] is replaced with FLP for all CLIP-based WSSS methods for fair comparisons.

4.2 Comparison with WSSS Methods

4.2.1 Evaluation of Pseudo Labels and Face Parsing. The first column of Tab. 1 reports the mean F1 scores of pseudo masks generated by DisFaceRep and recent WSSS baselines on the CelebAMask-HQ training subset. Our method achieves the highest score of 44.81%, significantly outperforming all competitors, including those using image-level supervision and those combining image-level and language supervision. Compared to SeCo [62], the strongest image-level WSSS baseline, DisFaceRep achieves a gain of 9.78%. Furthermore, it surpasses the best language-guided baseline, CLIP-ES [27], by a large margin of 20.24%, demonstrating the effectiveness of the proposed DisFaceRep in generating high-quality pseudo labels.

Fig. 3 compares the FCAMs generated by DisFaceRep with those from conventional WSSS methods for facial components exhibiting strong co-occurrence and visual similarity. DisFaceRep consistently activates more accurate and complete regions for challenging components such as skin and nose, as shown in the first two columns of Fig.3. In contrast, WSSS-based methods often miss these regions (e.g., SeCo [62], WeakCLIP [74]), underestimate them (e.g., MCTformer+ [60]), or falsely activate unrelated areas (e.g., MoRe [63],

Table 1: Mean F1 scores (%) of pseudo masks and face parsing results generated by the proposed method and existing WSSS methods on the CelebAMask-HQ training subset, validation, and testing sets. Back. denotes the backbone network. Sup. denotes the weak supervision type.

Methods	Back.	Sup.	Mask	val	test
MCTformer+ [60] [TPAMI24]	ViT-B	I	29.89	25.73	25.88
SeCo [62] [CVPR24]	ViT-B	I	35.03	24.31	24.64
MoRe [63] [AAAI25]	ViT-B	I	20.03	7.92	8.23
CLIMS [59] [CVPR22]	Res38	I+L	17.71	15.06	14.72
CLIP-ES [27] [CVPR23]	Res101	I+L	24.57	26.89	27.48
WeakCLIP [74] [IJCV24]	ViT-B	I+L	21.78	20.07	19.74
WeCLIP [65] [CVPR24]	ViT-B	I+L	22.67	19.73	20.37
WeCLIP+ [66] [TPAMI25]	ViT-B	I+L	18.55	18.18	18.29
DisFaceRep [Ours]	ViT-B	I+L	44.81	40.44	40.73

CLIP-ES [27]). Moreover, WSSS methods also struggle to distinguish symmetrical components such as left/right eyes, eyebrows, and ears—frequently activating them uniformly or mislocalizing them. DisFaceRep, on the other hand, maintains strong component-level discrimination. Fig. 5 further demonstrates that DisFaceRep also produces accurate activation for less frequently co-occurring attributes, including eyeglass, cloth, hat, earrings, and necklace.

We further evaluate our method by training a segmentation network—DeepLab-V1 [24] with ResNet38 [58]—on the CelebAMask-HQ training set. The face parsing results, shown in the second and

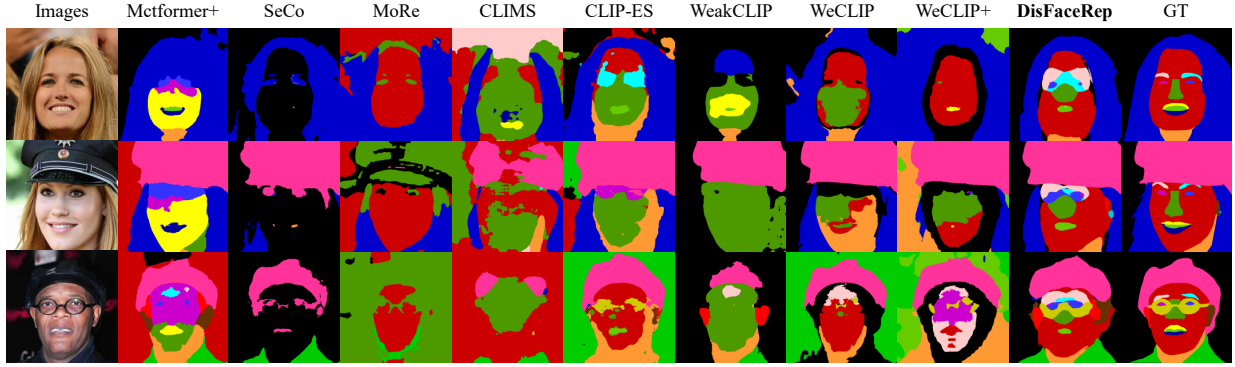


Figure 4: Qualitative comparison of face parsing results on CelebAMask-HQ between WSSS methods and DisFaceRep.

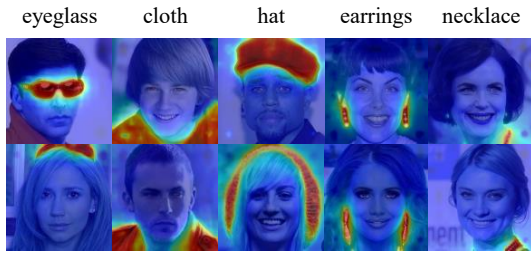


Figure 5: Qualitative comparison of FCAMs for less frequently co-occurring and visually distinctive facial components in the CelebAMask-HQ dataset.

third columns of Tab. 1, demonstrate that DisFaceRep achieves the best performance among all compared WSSS methods, with mean F1 scores of 40.44% on the validation set and 40.73% on the test set. Compared to MCTformer+, which uses only image-level supervision, DisFaceRep yields improvements of 14.71% and 14.85% on the validation and test sets, respectively. It also outperforms CLIMS, which incorporates both image-level and language supervision, by 25.38% and 26.01%. Qualitative results in Fig. 4 further confirm that DisFaceRep produces more accurate and compact segmentation maps than prior WSSS methods. While full activation of left and right attributes remains a challenge, our method significantly mitigates the co-occurrence issue.

4.2.2 Cross-Dataset Face Parsing. To assess cross-dataset generalization, we evaluate models trained on CelebAMask-HQ pseudo labels using the LaPa [33] and Helen [48] datasets. It is noted that the 19-category CelebAMask-HQ covers all 11 categories in LaPa and Helen. Hence, except for 8 extra classes, we can map the same 11 categories from CelebAMask-HQ to LaPa and Helen by indices (e.g., nose label: 2 \Rightarrow 6). Additionally, these datasets contain no overlapping images, preventing data leakage and ensuring valid cross-dataset evaluation. As shown in Tab. 2, DisFaceRep consistently achieves the highest performance across both datasets. On LaPa, it obtains 28.90% and 28.79% mean F1 scores on the validation and test sets, respectively, which is more than 10% higher than the next best method, CLIP-ES. On Helen, DisFaceRep also outperforms all baselines, reaching 26.83% on the validation set and 27.66% on the test set. These results demonstrate the strong cross-dataset generalization ability of DisFaceRep.

Table 2: Cross-dataset face parsing results on the LaPa and Helen datasets. Mean F1 scores (%) are reported on the validation and test sets.

Methods	LaPa [33]		Helen [48]	
	val	test	val	test
MCTformer+ [60] [TPAMI24]	11.30	11.08	12.14	13.12
SeCo [62] [CVPR24]	10.32	10.40	10.67	11.21
MoRe [63] [AAAI25]	5.34	5.39	6.13	7.06
CLIMS [59] [CVPR22]	6.60	6.38	6.35	7.01
CLIP-ES [27] [CVPR23]	18.44	18.50	19.01	19.60
WeakCLIP [74] [IJCV24]	5.98	5.70	6.75	7.69
WeCLIP [65] [CVPR24]	12.81	12.85	13.14	13.29
WeCLIP+ [66] [TPAMI25]	14.09	13.92	12.15	12.65
DisFaceRep [Ours]	28.90	28.79	26.83	27.66

Table 3: Ablation studies of component disentanglement modules of CCD and TCD on CelebAMask-HQ training subset. The results above are based on pseudo labels. Base. denotes the baseline model.

Methods	skin	nose	r-eye	r-brow	l-ear	Mean F1
Base.	14.65	10.68	1.15	11.42	6.00	29.67
Base.+CCD	30.87	47.41	3.71	10.20	6.80	33.86
Base.+CCD+TCD	72.68	73.14	22.55	19.31	26.65	44.81

4.3 Ablation Studies and Analysis

4.3.1 Effectiveness of CCD and TCD Modules. We conduct ablation studies on the CelebAMask-HQ training subset to evaluate the effectiveness of the proposed CCD and TCD modules for pseudo label generation. As shown in Tab. 3, the baseline model without CCD and TCD modules achieves a mean F1 score of 29.67%. Incorporating CCD alone improves the score to 33.86%, demonstrating the effectiveness of suppressing frequently co-occurring facial components to reduce feature entanglement and improve activation quality. Adding TCD further boosts performance to 44.81%, demonstrating the effectiveness of text-guided component disentanglement. We also report the results for frequently co-occurring facial attributes (e.g., skin, nose, right eye, right eyebrow, and left ear). The results show that combining CCD and TCD in DisFaceRep significantly improves prediction accuracy for these challenging components.

Table 4: Comparison of the quality of pseudo labels using different combinations of loss functions. The mean F1 scores are reported on the CelebAMask-HQ training subset.

L_{pos}^{cls}	L_{pos}^{ffc}	L_{neg}^{cls}	L_{neg}^{ffc}	L_{neg}^{bfc}	L_{reg}	Mean F1
✓						35.01
✓	✓					36.37
✓	✓	✓				37.49
✓	✓	✓	✓			41.17
✓	✓	✓	✓	✓		41.21
✓	✓	✓	✓	✓	✓	44.81

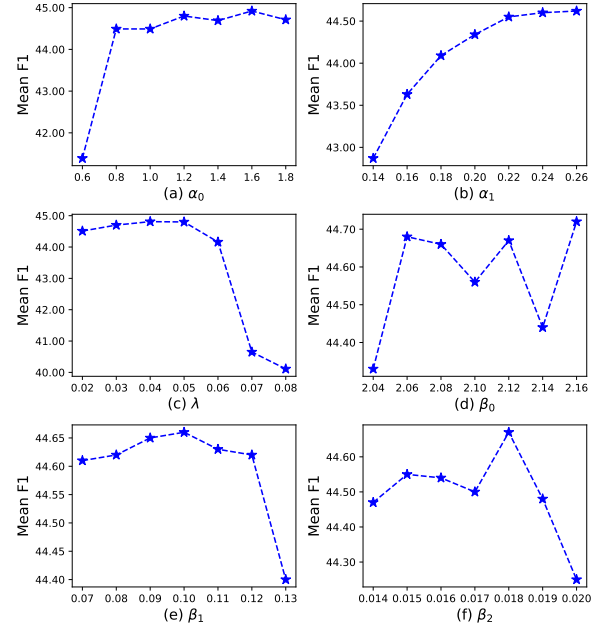
Table 5: Comparison of model complexity and training efficiency with image size 448×448 .

Methods	Train Params↓	Total Params↓	Train Time↓	MACs↓	FPS↑
SeCo [62]	94.9 M	189.6 M	8.2 h	67.6 G	44.2
WeCLIP [65]	16.2 M	155.6 M	4.4 h	45.27 G	106.1
MCTformer+ [60]	22.0 M	22.0 M	2.3 h	17.3 G	159.5
DisFaceRep	22.5 M	172.1 M	4.3 h	17.3 G	142.4

4.3.2 Impact of Loss Functions on TCD. We conduct an ablation study on the CelebAMask-HQ training subset to evaluate the effectiveness of each loss function in the TCD module. As shown in Tab. 4, using only the class-text positive loss \mathcal{L}_{pos}^{cls} yields a baseline mean F1 score of 35.01%. This already surpasses the baseline using only image-level supervision (29.67% in Tab.3), demonstrating the benefit of text-guided supervision in WSFP. Adding the foreground-level positive loss \mathcal{L}_{pos}^{ffc} further improves the mean F1 score to 36.37%, showing that both positive terms contribute to more accurate component activation. Introducing the class-text negative loss \mathcal{L}_{neg}^{cls} raises performance to 37.49%, while including all three negative losses (\mathcal{L}_{neg}^{cls} , \mathcal{L}_{neg}^{ffc} , and \mathcal{L}_{neg}^{bfc}) boosts the score to 41.21%. Finally, adding the regularization term \mathcal{L}_{reg} results in the highest performance of 44.81%, indicating that enforcing spatial compactness in activation maps further enhances pseudo label quality. These results highlight the complementary roles of each loss and validate the effectiveness of the full TCD loss design in generating accurate and discriminative FCAMs.

4.3.3 Sensitivity and Complexity Analysis. We conduct sensitivity analysis on hyperparameters in DisFaceRep: α_0 , α_1 , β_0 , β_1 , β_2 , and λ , corresponding to Eq.10, Eq.14, and Eq. 16, using pseudo label generation on the CelebAMask-HQ training subset. As shown in Fig.6(a) and (b), the mean F1 score remains stable as α_0 varies from 0.8 to 1.8 and α_1 from 0.20 to 0.26, indicating robustness to the positive alignment weights. In Fig.6(c), varying λ between 0.02 and 0.06 has minimal effect, confirming the stability of the regularization term. Fig. 6(d)–(f) show that the mean F1 scores remain consistently around 44% as β_0 , β_1 , and β_2 vary within [2.06, 2.16], [0.07, 0.12], and [0.014, 0.019], respectively. These results show that DisFaceRep is robust to hyperparameter choices across a wide range of values.

Tab. 5 shows the model complexity and training efficiency of our DisFaceRep, SeCo [62], WeCLIP [65], and MCTformer+ [60]. It is worth noting that Grounding DINO [32] is used before training, and FLIP [22] is frozen in training and removed during inference

**Figure 6: Sensitivity analysis on α_0 , α_1 , λ , β_0 , β_1 , and β_2 . Mean F1 scores for pseudo-labels are reported on the CelebAMask-HQ training subset.**

in DisFaceRep. Therefore, our DisFaceRep has similar complexity and computational costs in terms of trainable and total parameters, training time, MACs, and FPS compared to the comparison methods.

4.3.4 Impact of Language-Image Pre-training Models. We evaluate the impact of different vision-language pretraining models, namely CLIP [43] and FLIP [22], on DisFaceRep. Using CLIP results in a mean F1 score of 37.20% for pseudo-labeling on the CelebAMask-HQ training subset, while FLIP achieves a significantly higher score of 44.81%. This 7.61% improvement demonstrates the effectiveness of domain-specific pretraining. As FLIP is fine-tuned on facial image-text pairs, it provides stronger semantic alignment for facial components, leading to more accurate pseudo label generation. These results highlight the importance of choosing a vision-language model that is well-aligned with the task domain.

5 Conclusion

We introduced Weakly Supervised Face Parsing (WSFP), a new task that focuses on segmenting facial components using only weak supervision. WSFP presents unique challenges due to the frequent co-occurrence and high visual similarity of facial attributes. To address this, we proposed DisFaceRep, a representation disentanglement framework that explicitly suppresses dominant components via co-occurring component disentanglement and implicitly enhances component separation through text-guided alignment. Extensive experiments demonstrate that DisFaceRep generates more complete and compact activation maps compared to existing weakly supervised semantic segmentation methods. Cross-dataset evaluations further confirm its strong generalization ability, validating the effectiveness of disentangling co-occurring facial components for robust weakly supervised face parsing.

Acknowledgments

This work was supported by the National Natural Science Foundation of China under Grants 82261138629 and 62206180, Guangdong Basic and Applied Basic Research Foundation under Grant 2023A1515010688, Guangdong Provincial Key Laboratory under Grant 2023B1212060076, Shenzhen Municipal Science and Technology Innovation Council under Grant JCYJ20220531101412030, and XJTLU Research Development Funds under Grant RDF-23-01-053.

References

- [1] Jiwoon Ahn, Sunghyun Cho, and Suha Kwak. 2019. Weakly supervised learning of instance segmentation with inter-pixel relations. In *Proceedings of the IEEE/CVF conference on computer vision and pattern recognition*. 2209–2218.
- [2] Jiwoon Ahn and Suha Kwak. 2018. Learning pixel-level semantic affinity with image-level supervision for weakly supervised semantic segmentation. In *Proceedings of the IEEE conference on computer vision and pattern recognition*. 4981–4990.
- [3] Amy Bearman, Olga Russakovsky, Vittorio Ferrari, and Li Fei-Fei. 2016. What's the point: Semantic segmentation with point supervision. In *European conference on computer vision*. Springer, 549–565.
- [4] Liang-Chieh Chen, George Papandreou, Iasonas Kokkinos, Kevin Murphy, and Alan L Yuille. 2014. Semantic image segmentation with deep convolutional nets and fully connected crfs. *arXiv preprint arXiv:1412.7062* (2014).
- [5] Zhaozheng Chen, Tan Wang, Xiongwei Wu, Xian-Sheng Hua, Hanwang Zhang, and Qianru Sun. 2022. Class re-activation maps for weakly-supervised semantic segmentation. In *Proceedings of the IEEE/CVF conference on computer vision and pattern recognition*. 969–978.
- [6] Jifeng Dai, Kaiming He, and Jian Sun. 2015. Boxsup: Exploiting bounding boxes to supervise convolutional networks for semantic segmentation. In *Proceedings of the IEEE international conference on computer vision*. 1635–1643.
- [7] Jia Deng, Wei Dong, Richard Socher, Li-Jia Li, Kai Li, and Li Fei-Fei. 2009. Imagenet: A large-scale hierarchical image database. In *2009 IEEE conference on computer vision and pattern recognition*. Ieee, 248–255.
- [8] Alexey Dosovitskiy, Lucas Beyer, Alexander Kolesnikov, Dirk Weissenborn, Xi-aohua Zhai, Thomas Unterthiner, Mostafa Dehghani, Matthias Minderer, Georg Heigold, Sylvain Gelly, et al. 2020. An image is worth 16x16 words: Transformers for image recognition at scale. *arXiv preprint arXiv:2010.11929* (2020).
- [9] Mark Everingham, Luc Van Gool, Christopher KI Williams, John Winn, and Andrew Zisserman. 2010. The pascal visual object classes (voc) challenge. *International journal of computer vision* 88 (2010), 303–338.
- [10] Junsong Fan, Zhaoxiang Zhang, Chunfeng Song, and Tieniu Tan. 2020. Learning integral objects with intra-class discriminator for weakly-supervised semantic segmentation. In *Proceedings of the IEEE/CVF conference on computer vision and pattern recognition*. 4283–4292.
- [11] Tianchu Guo, Youngsuk Kim, Hui Zhang, Deheng Qian, ByungIn Yoo, Jingtao Xu, Dongqing Zou, Jae-Joon Han, and Changkyu Choi. 2018. Residual encoder decoder network and adaptive prior for face parsing. In *Proceedings of the AAAI Conference on Artificial Intelligence*, Vol. 32.
- [12] Aaron S Jackson, Michel Valstar, and Georgios Tzimiropoulos. 2016. A CNN cascade for landmark guided semantic part segmentation. In *Computer Vision—ECCV 2016 Workshops: Amsterdam, The Netherlands, October 8–10 and 15–16, 2016, Proceedings, Part III 14*. Springer, 143–155.
- [13] Peng-Tao Jiang, Qibin Hou, Yang Cao, Ming-Ming Cheng, Yunchao Wei, and Hong-Kai Xiong. 2019. Integral object mining via online attention accumulation. In *Proceedings of the IEEE/CVF international conference on computer vision*. 2070–2079.
- [14] Sanghyun Jo, In-Jae Yu, and Kyungsu Kim. 2022. Recurseed and edgepredictmix: Single-stage learning is sufficient for weakly-supervised semantic segmentation. *arXiv preprint arXiv:2204.06754* (2022).
- [15] Sanghyun Jo, In-Jae Yu, and Kyungsu Kim. 2023. MARS: Model-agnostic biased object removal without additional supervision for weakly-supervised semantic segmentation. In *Proceedings of the IEEE/CVF International Conference on Computer Vision*. 614–623.
- [16] Alexander Kolesnikov and Christoph H Lampert. 2016. Seed, expand and constrain: Three principles for weakly-supervised image segmentation. In *Computer Vision—ECCV 2016: 14th European Conference, Amsterdam, The Netherlands, October 11–14, 2016, Proceedings, Part IV 14*. Springer, 695–711.
- [17] Philipp Krähenbühl and Vladlen Koltun. 2011. Efficient inference in fully connected crfs with gaussian edge potentials. *Advances in neural information processing systems* 24 (2011).
- [18] Hyeokjun Kwon, Sung-Hoon Yoon, Hyeonseong Kim, Dahee Park, and Kuk-Jin Yoon. 2021. Unlocking the potential of ordinary classifier: Class-specific adversarial erasing framework for weakly supervised semantic segmentation. In *Proceedings of the IEEE/CVF international conference on computer vision*. 6994–7003.
- [19] Hyeokjun Kwon, Sung-Hoon Yoon, and Kuk-Jin Yoon. 2023. Weakly supervised semantic segmentation via adversarial learning of classifier and reconstructor. In *Proceedings of the IEEE/CVF Conference on Computer Vision and Pattern Recognition*. 11329–11339.
- [20] Cheng-Han Lee, Ziwei Liu, Lingyun Wu, and Ping Luo. 2020. Maskgan: Towards diverse and interactive facial image manipulation. In *Proceedings of the IEEE/CVF conference on computer vision and pattern recognition*. 5549–5558.
- [21] Xueyi Li, Tianfei Zhou, Jianwu Li, Yi Zhou, and Zhaoxiang Zhang. 2021. Group-wise semantic mining for weakly supervised semantic segmentation. In *Proceedings of the AAAI conference on artificial intelligence*, Vol. 35. 1984–1992.
- [22] Yudong Li, Xianxu Hou, Dezhi Zheng, Linlin Shen, and Zhe Zhao. 2024. FLIP-80M: 80 Million Visual-Linguistic Pairs for Facial Language-Image Pre-Training. In *ACM Multimedia 2024*.
- [23] Yijun Li, Sifei Liu, Jimei Yang, and Ming-Hsuan Yang. 2017. Generative face completion. In *Proceedings of the IEEE conference on computer vision and pattern recognition*. 3911–3919.
- [24] Chen Liang-Chieh, George Papandreou, Iasonas Kokkinos, Kevin Murphy, and Alan Yuille. 2015. Semantic image segmentation with deep convolutional nets and fully connected crfs. In *International conference on learning representations*.
- [25] Di Lin, Jifeng Dai, Jiayia Jia, Kaiming He, and Jian Sun. 2016. Scribblesup: Scribble-supervised convolutional networks for semantic segmentation. In *Proceedings of the IEEE conference on computer vision and pattern recognition*. 3159–3167.
- [26] Jinpeng Lin, Hao Yang, Dong Chen, Ming Zeng, Fang Wen, and Lu Yuan. 2019. Face parsing with roi tanh-warping. In *Proceedings of the IEEE/CVF Conference on Computer Vision and Pattern Recognition*. 5654–5663.
- [27] Yuqi Lin, Minghao Chen, Wenxiao Wang, Boxi Wu, Ke Li, Binbin Lin, Haifeng Liu, and Xiaofei He. 2023. Clip is also an efficient segmenter: A text-driven approach for weakly supervised semantic segmentation. In *Proceedings of the IEEE/CVF Conference on Computer Vision and Pattern Recognition*. 15305–15314.
- [28] Yiming Lin, Jie Shen, Yujiang Wang, and Maja Pantic. 2021. Roi tanh-polar transformer network for face parsing in the wild. *Image and Vision Computing* 112 (2021), 104190.
- [29] Sifei Liu, Jianping Shi, Ji Liang, and Ming-Hsuan Yang. 2017. Face parsing via recurrent propagation. *arXiv preprint arXiv:1708.01936* (2017).
- [30] Sifei Liu, Jimei Yang, Chang Huang, and Ming-Hsuan Yang. 2015. Multi-objective convolutional learning for face labeling. In *Proceedings of the IEEE conference on computer vision and pattern recognition*. 3451–3459.
- [31] Shilong Liu, Zhaoxiang Zeng, Tianhe Ren, Feng Li, Hao Zhang, Jie Yang, Qing Jiang, Chunyuan Li, Jianwei Yang, Hang Su, et al. 2024. Grounding dino: Marrying dino with grounded pre-training for open-set object detection. In *European Conference on Computer Vision*. Springer, 38–55.
- [32] Shilong Liu, Zhaoxiang Zeng, Tianhe Ren, Feng Li, Hao Zhang, Jie Yang, Qing Jiang, Chunyuan Li, Jianwei Yang, Hang Su, et al. 2025. Grounding dino: Marrying dino with grounded pre-training for open-set object detection. In *European Conference on Computer Vision*. Springer, 38–55.
- [33] Yinglu Liu, Hailin Shi, Hao Shen, Yue Si, Xiaobo Wang, and Tao Mei. 2020. A new dataset and boundary-attention semantic segmentation for face parsing. In *Proceedings of the AAAI Conference on Artificial Intelligence*, Vol. 34. 11637–11644.
- [34] Yun Liu, Yu-Huan Wu, Peisong Wen, Yujun Shi, Yu Qiu, and Ming-Ming Cheng. 2020. Leveraging instance-, image- and dataset-level information for weakly supervised instance segmentation. *IEEE Transactions on Pattern Analysis and Machine Intelligence* 44, 3 (2020), 1415–1428.
- [35] Ling Luo, Dingyu Xue, and Xinglong Feng. 2020. Ehanet: An effective hierarchical aggregation network for face parsing. *Applied Sciences* 10, 9 (2020), 3135.
- [36] Ping Luo, Xiaogang Wang, and Xiaoou Tang. 2012. Hierarchical face parsing via deep learning. In *2012 IEEE Conference on Computer Vision and Pattern Recognition*. IEEE, 2480–2487.
- [37] Kartik Narayan, Vibashan VS, and Vishal M Patel. 2025. SegFace: Face Segmentation of Long-Tail Classes. In *Proceedings of the AAAI Conference on Artificial Intelligence*.
- [38] Yuval Nirkin, Yosi Keller, and Tal Hassner. 2019. Fsgan: Subject agnostic face swapping and reenactment. In *Proceedings of the IEEE/CVF international conference on computer vision*. 7184–7193.
- [39] Xinyu Ou, Si Liu, Xiaochun Cao, and Hefei Ling. 2016. Beauty emakeup: A deep makeup transfer system. In *Proceedings of the 24th ACM international conference on Multimedia*. 701–702.
- [40] George Papandreou, Liang-Chieh Chen, Kevin P Murphy, and Alan L Yuille. 2015. Weakly-and semi-supervised learning of a deep convolutional network for semantic image segmentation. In *Proceedings of the IEEE international conference on computer vision*. 1742–1750.
- [41] Deepak Pathak, Philipp Krähenbühl, and Trevor Darrell. 2015. Constrained convolutional neural networks for weakly supervised segmentation. In *Proceedings of the IEEE international conference on computer vision*. 1796–1804.
- [42] Pedro O Pinheiro and Ronan Collobert. 2015. From image-level to pixel-level labeling with convolutional networks. In *Proceedings of the IEEE conference on computer vision and pattern recognition*. 1713–1721.
- [43] Alec Radford, Jong Wook Kim, Chris Hallacy, Aditya Ramesh, Gabriel Goh, Sandhini Agarwal, Girish Sastry, Amanda Askell, Pamela Mishkin, Jack Clark,

- et al. 2021. Learning transferable visual models from natural language supervision. In *International conference on machine learning*. PmlR, 8748–8763.
- [44] Shenghai Rong, Bohai Tu, Zilei Wang, and Junjie Li. 2023. Boundary-enhanced co-training for weakly supervised semantic segmentation. In *Proceedings of the IEEE/CVF Conference on Computer Vision and Pattern Recognition*. 19574–19584.
- [45] Simone Rossetti, Damiano Zappia, Marta Sanzari, Marco Schaerf, and Fiora Pirri. 2022. Max pooling with vision transformers reconciles class and shape in weakly supervised semantic segmentation. In *European conference on computer vision*. Springer, 446–463.
- [46] Mausoom Sarkar, Mayur Hemani, Rishabh Jain, Balaji Krishnamurthy, et al. 2023. Parameter efficient local implicit image function network for face segmentation. In *Proceedings of the IEEE/CVF Conference on Computer Vision and Pattern Recognition*. 20970–20980.
- [47] Ramprasaath R Selvaraju, Michael Cogswell, Abhishek Das, Ramakrishna Vedantam, Devi Parikh, and Dhruv Batra. 2017. Grad-cam: Visual explanations from deep networks via gradient-based localization. In *Proceedings of the IEEE international conference on computer vision*. 618–626.
- [48] Brandon M Smith, Li Zhang, Jonathan Brandt, Zhe Lin, and Jianchao Yang. 2013. Exemplar-based face parsing. In *Proceedings of the IEEE conference on computer vision and pattern recognition*. 3484–3491.
- [49] Guolei Sun, Wenguan Wang, Jifeng Dai, and Luc Van Gool. 2020. Mining cross-image semantics for weakly supervised semantic segmentation. In *Computer Vision—ECCV 2020: 16th European Conference, Glasgow, UK, August 23–28, 2020, Proceedings, Part II* 16. Springer, 347–365.
- [50] Gusi Te, Wei Hu, Yinglu Liu, Hailin Shi, and Tao Mei. 2021. Agrnet: Adaptive graph representation learning and reasoning for face parsing. *IEEE Transactions on Image Processing* 30 (2021), 8236–8250.
- [51] Gusi Te, Yinglu Liu, Wei Hu, Hailin Shi, and Tao Mei. 2020. Edge-aware graph representation learning and reasoning for face parsing. In *Computer Vision—ECCV 2020: 16th European Conference, Glasgow, UK, August 23–28, 2020, Proceedings, Part XII* 16. Springer, 258–274.
- [52] Hugo Touvron, Matthieu Cord, Matthijs Douze, Francisco Massa, Alexandre Sablayrolles, and Hervé Jégou. 2021. Training data-efficient image transformers & distillation through attention. In *International conference on machine learning*. PMLR, 10347–10357.
- [53] Paul Vernaza and Manmohan Chandraker. 2017. Learning random-walk label propagation for weakly-supervised semantic segmentation. In *Proceedings of the IEEE conference on computer vision and pattern recognition*. 7158–7166.
- [54] Yude Wang, Jie Zhang, Meina Kan, Shiguang Shan, and Xilin Chen. 2020. Self-supervised equivariant attention mechanism for weakly supervised semantic segmentation. In *Proceedings of the IEEE/CVF conference on computer vision and pattern recognition*. 12275–12284.
- [55] Zhen Wei, Yao Sun, Jinqiao Wang, Hanjiang Lai, and Si Liu. 2017. Learning adaptive receptive fields for deep image parsing network. In *Proceedings of the IEEE conference on computer vision and pattern recognition*. 2434–2442.
- [56] Tong Wu, Guangyu Gao, Junshi Huang, Xiaolin Wei, Xiaoming Wei, and Chi Harold Liu. 2022. Adaptive spatial-bce loss for weakly supervised semantic segmentation. In *European Conference on Computer Vision*. Springer, 199–216.
- [57] Yuanchen Wu, Xichen Ye, Kequan Yang, Jide Li, and Xiaoqiang Li. 2024. DuPL: Dual Student with Trustworthy Progressive Learning for Robust Weakly Supervised Semantic Segmentation. In *Proceedings of the IEEE/CVF Conference on Computer Vision and Pattern Recognition*. 3534–3543.
- [58] Zifeng Wu, Chunhua Shen, and Anton Van Den Hengel. 2019. Wider or deeper: Revisiting the resnet model for visual recognition. *Pattern recognition* 90 (2019), 119–133.
- [59] Jinheng Xie, Xianxu Hou, Kai Ye, and Linlin Shen. 2022. Clims: Cross language image matching for weakly supervised semantic segmentation. In *Proceedings of the IEEE/CVF conference on computer vision and pattern recognition*. 4483–4492.
- [60] Lian Xu, Mohammed Bennamoun, Farid Boussaid, Hamid Laga, Wanli Ouyang, and Dan Xu. 2024. Mctformer+: Multi-class token transformer for weakly supervised semantic segmentation. *IEEE transactions on pattern analysis and machine intelligence* (2024).
- [61] Lian Xu, Wanli Ouyang, Mohammed Bennamoun, Farid Boussaid, and Dan Xu. 2022. Multi-class token transformer for weakly supervised semantic segmentation. In *Proceedings of the IEEE/CVF conference on computer vision and pattern recognition*. 4310–4319.
- [62] Zhiwei Yang, Kexue Fu, Minghong Duan, Linhao Qu, Shuo Wang, and Zhijian Song. 2024. Separate and conquer: Decoupling co-occurrence via decomposition and representation for weakly supervised semantic segmentation. In *Proceedings of the IEEE/CVF Conference on Computer Vision and Pattern Recognition*. 3606–3615.
- [63] Zhiwei Yang, Yucong Meng, Kexue Fu, Shuo Wang, and Zhijian Song. 2025. MoRe: Class Patch Attention Needs Regularization for Weakly Supervised Semantic Segmentation. In *Proceedings of the AAAI Conference on Artificial Intelligence*.
- [64] Sung-Hoon Yoon, Hyeokjun Kwon, Jegyeong Cho, Shinjeong Kim, and Kuk-Jin Yoon. 2022. Adversarial erasing framework via triplet with gated pyramid pooling layer for weakly supervised semantic segmentation. In *European Conference on Computer Vision*. Springer, 326–344.
- [65] Bingfeng Zhang, Siyue Yu, Yunchao Wei, Yao Zhao, and Jimin Xiao. 2024. Frozen CLIP: A Strong Backbone for Weakly Supervised Semantic Segmentation. In *Proceedings of the IEEE/CVF Conference on Computer Vision and Pattern Recognition*. 3796–3806.
- [66] Bingfeng Zhang, Siyue Yu, Jimin Xiao, Yunchao Wei, and Yao Zhao. 2025. Frozen CLIP-DINO: a Strong Backbone for Weakly Supervised Semantic Segmentation. *IEEE Transactions on Pattern Analysis and Machine Intelligence* (2025).
- [67] Fei Zhang, Chaochen Gu, Chenyue Zhang, and Yuchao Dai. 2021. Complementary patch for weakly supervised semantic segmentation. In *Proceedings of the IEEE/CVF international conference on computer vision*. 7242–7251.
- [68] Xiaolin Zhang, Yunchao Wei, Jiashi Feng, Yi Yang, and Thomas S Huang. 2018. Adversarial complementary learning for weakly supervised object localization. In *Proceedings of the IEEE conference on computer vision and pattern recognition*. 1325–1334.
- [69] Qingping Zheng, Jiankang Deng, Zheng Zhu, Ying Li, and Stefanos Zafeiriou. 2022. Decoupled multi-task learning with cyclical self-regulation for face parsing. In *Proceedings of the IEEE/CVF conference on computer vision and pattern recognition*. 4156–4165.
- [70] Yinglin Zheng, Hao Yang, Ting Zhang, Jianmin Bao, Dongdong Chen, Yangyu Huang, Lu Yuan, Dong Chen, Ming Zeng, and Fang Wen. 2022. General facial representation learning in a visual-linguistic manner. In *Proceedings of the IEEE/CVF conference on computer vision and pattern recognition*. 18697–18709.
- [71] Bolei Zhou, Aditya Khosla, Agata Lapedriza, Aude Oliva, and Antonio Torralba. 2016. Learning deep features for discriminative localization. In *Proceedings of the IEEE conference on computer vision and pattern recognition*. 2921–2929.
- [72] Lei Zhou, Zhi Liu, and Xiangjian He. 2017. Face parsing via a fully-convolutional continuous CRF neural network. *arXiv preprint arXiv:1708.03736* (2017).
- [73] Yisu Zhou, Xiaolin Hu, and Bo Zhang. 2015. Interlinked convolutional neural networks for face parsing. In *Advances in Neural Networks—ISNN 2015: 12th International Symposium on Neural Networks, ISNN 2015, Jeju, South Korea, October 15–18, 2015, Proceedings* 12. Springer, 222–231.
- [74] Lianghui Zhu, Xinggang Wang, Jiawei Feng, Tianheng Cheng, Yingyue Li, Bo Jiang, Dingwen Zhang, and Junwei Han. 2024. WeakCLIP: Adapting CLIP for Weakly-Supervised Semantic Segmentation. *International Journal of Computer Vision* (2024), 1–21.